Sensitivity enhancement of thermal lens spectrometry

Dy, Eben; Gu, Caikang; Shen, Jun; Qu, Wei; Xie, Zhong; Wang, Xiaomeng; Baesso, Mauro L.; Astrath, Nelson G. C.

Publisher's version / Version de l'éditeur:
https://doi.org/10.1063/5.0083080
Journal of Applied Physics, 131, 6, pp. 1-5, 2022-02-10

Sensitivity enhancement of thermal lens spectrometry

Eben Dy[1], Caikang Gu[1], Jun Shen[1], Wei Qu[1], Zhong Xie[1], Xiaomeng Wang[2], Mauro L. Baesso[3], Nelson G. C. Astrath[3]*

[1]National Research Council Canada, Energy, Mining and Environment Research Centre, 4250 Wesbrook Mall, Vancouver, British Columbia V6T 1W5, Canada

[2]Natural Resources Canada, CanmetENERGY in Devon, One Oil Drive Patch, Devon, Alberta T9G 1A8, Canada

[3]Departamento de Física, Universidade Estadual de Maringá, Maringá, PR 87020-900, Brazil

* Author to whom correspondence should be addressed: jun.shen@nrc-cnrc.gc.ca

ABSTRACT

Thermal lens spectrometry has been utilized in various applications, and in some application areas high sensitivity is required. In this work, a mode-mismatched thermal lens configuration probing thermal lens twice was developed for sensitivity enhancement. Experimental results exhibited that doubled sensitivity was achieved with this configuration compared with that attained with a conventional one, which was consistent with the prediction of the theoretical model for thermal lens spectrometry. As a result of the consistency, the linear absorption (attenuation) coefficient of deionized water at 532.3 nm was directly measured with this configuration and the conventional one, and found to be $(4.90 \pm 0.05) \times 10^{-2}$ m^{-1} and $(4.7 \pm 0.2) \times 10^{-2}$ m^{-1} respectively. The results are in good agreement with accepted literature values. Theoretical analysis revealed that the sensitivity enhancement with this configuration is greater than that by simply doubling the sample thickness in a conventional configuration.

I. INTRODUCTION

Thermal lens effect is the foundation of the widely applied thermal lens spectrometry. When a TEM_{00} Gaussian profile laser beam (the excitation beam, EB) illuminates a semi-transparent sample, the sample is heated by the absorbed laser energy, and a radial temperature gradient is established. Since the refractive index of the sample changes with temperature, a radial refractive-index gradient is created, forming a lens-like optical element — the so-called thermal lens (TL). The propagation of a TEM_{00} Gaussian laser beam (the probe beam, PB) passing through the TL will be affected: an optical path length change to the probe beam is introduced, which can be expressed as an additional phase shift on the PB wavefront, resulting in the variation of the spot size and then intensity distribution of the PB. The information on the optical and thermophysical properties of the sample can then be obtained by measuring these variations.

Thermal lens spectrometry has been utilized in various applications,[1-4] and in some of those, e.g., ultra-trace analysis,[5] high sensitivity is required.[6] Considerable efforts have been made to improve the sensitivity. Early experimental devices used one laser beam to excite and probe the TL. Hu and Whinnery demonstrated that a sensitive thermal lens detection could be achieved using a converging lens to form a beam waist at one confocal distance (namely, Rayleigh length) before the sample.[7] Later, dual-beam experimental arrangements emerged, which used separate laser beams for exciting and probing the TL.[8] There are two kinds of dual-beam TL experimental arrangements. One is mode-matched, in which the spot sizes of the EB and PB in the sample are the same. The other is mode-mismatched, wherein the spot sizes are different. The mode-mismatched arrangement was found to be more sensitive than the mode-matched one.[9] Berthoud et al. discussed the significance of the beam geometric positions in a mode-mismatched experiment.[10] In their experiments, the maximum steady-state TL signal was obtained when the

sample was placed at the $\sqrt{3}$ confocal distance related to the PB waist and at the waist of the focused EB, where the power density of the EB and the thermally produced refractive-index gradient were at a maximum. However, after analyzing the theoretical model for TL spectrometry presented in Ref. 11, Silva et al. pointed out that the optimized position of the sample is at $\sqrt{1+2m}$ confocal distance related to the PB waist and at the waist of the EB.[12] Here m is the square of the ratio of the spot size of the EB to that of the PB at the sample position. In a mode-matched TL experimental arrangement, $m = 1$ and $\sqrt{1+2m} = \sqrt{3}$. Taking full advantage of geometric and spatial aspects of a mode-mismatched configuration, Marcano et al. maximized the TL signal using an expanded and collimated PB, while the sample was located at the waist of a focused EB.[13] With a collimated PB and a focused EB, Cabrera et al. put a 1-mm-thick sample of Fe(II) - 1,10-Phenanthroline water/ethanol (80/20 v/v) solution in a 4-mm-long multi-pass optical cavity formed by two dichroic mirrors, in which one mirror was slightly inclined relating to the other.[14] The multiple reflections of the PB caused its multiple passes through the TL, which resulted in a significant TL signal enhancement. Calibration curves were measured and found that the slopes from the 2-passes and 10-passes were 1.9 and 9.1 times, respectively, of the slope of 1-pass. However, the enhancements were less than 2 and 10 times, respectively, as predicted by the theoretical model for TL spectrometry because of the walk-off of the PB in the multi-pass optical cavity and the deviation of the PB from the collimation in the multi-pass configuration.[14]

In this work, with a focused EB, a collimated PB is employed to probe TL twice, which is less complicated in construction and optical alignment compared with the multi-pass optical cavity. Experimental results exhibit that the sensitivity of this method is two-times of that of the conventional configuration (probing TL once), which is consistent with the prediction by the TL theoretical model. As a result of the consistency, the model can be employed to process

experimental data, and the linear absorption (or attenuation) coefficient can be measured straightforwardly for a sample whose thermophysical properties are well known. Moreover, this method can be applied to a thick sample (> 1 mm) to further enhance the sensitivity.

II. Method

In this work two TL experimental setups were used as shown in Fig. 1. In the conventional configuration (probing TL once), Fig. 1(a), the EB (Spectra-Physics, Excelsior-532-200-CDRH, 532.3 ± 0.3 nm, maximum power 200 mW) was focused by a convex lens L_1 (focus length f = 100 mm), and the sample S was positioned at the EB waist. The PB (THORLABS, HRS015B, 632.992 nm, 1.5 mW) was expanded and collimated by a pair of plano-convex lenses L_2 (f = 25 mm) and L_3 (f = 200 mm). The collimated PB was partially reflected by a 50:50 non-polarizing beam splitter BS and contra-propagated collinearly with the EB. After probing the TL in the sample produced by EB illumination controlled by an optical beam shutter ST (THORLABS, SH05 driven by a shutter controller SC10), the PB was reflected by a dichroic mirror DM1 (THORLABS, DMSP567) to a pinhole-photodiode PH-PD assembly. A He-Ne laser line filter F was placed before the pinhole to prevent stray light entering the photodiode. The TL signal detected by the photodiode PD (THORLABS, DET100A) was magnified by a current amplifier AMP (Stanford Research System, SR570), which output was coupled to a digital oscilloscope DOS (Tektronix, TDS 3052). The diameter of the pinhole PH was 100 μm. The dichroic mirror DM2 (THORLABS, DMLP567) was employed to stop the EB entering the PB.

Different from the conventional configuration Fig. 1(a), after probing the TL, in the new configuration developed in this work as shown in Fig. 1(b), the PB was immediately reflected by the dichroic mirror DM1 to probe the TL once again. Reflected by a mirror M, the PB after probing

the TL twice was detected by the pinhole-photodiode assembly. It is crucial to properly adjust the DM1 to reflect the PB passing through the TL and propagating collinearly with the EB.

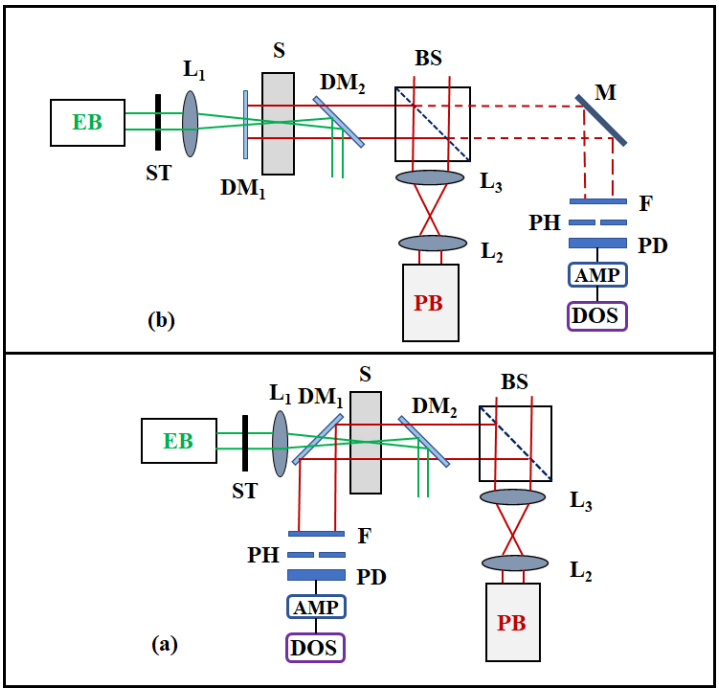

FIG. 1. Schematic diagrams of two TL experimental setups: (a) conventional configuration (probing TL once), (b) new configuration (probing TL twice). EB: 532.3 nm, PB: 632.992 nm, BS: beam splitter, L_i: lenses (i = 1, 2, 3), M: mirror, ST: optical beam shutter, S: sample, F: He-Ne laser line filter, PH: pinhole; PD: photodiode, DM1: dichroic mirror, DM2: dichroic mirror, AMP: current amplifier, DOS: digital oscilloscope

It is necessary to measure EB and PB spot sizes at the sample position for the comparison of experimental results with TL theory. A measurement of the location and spot size (i.e., radius) of EB waist was made following the approach reported in Ref. 11. A pinhole of a diameter $d = 15\ \mu m$ was placed before a Si switchable gain detector (THORLABS, PDA36A2), which was

connected to a multimeter. The pinhole-detector assembly was centred in the EB and moved along the EB path (Z direction). A plot of the power P_{de} thus detected versus Z was employed for a least-squares curve fitting to find the radius ω_e and location Z_0 of the EB waist. For the Gaussian EB of total power P_e and a radius $\omega(Z)$, the intensity distribution $I_e(r,Z)$ is[11]

$$I_e(r,Z) = \frac{2P_e}{\pi\omega^2(Z)} exp\left[-\frac{2r^2}{\omega^2(Z)}\right]. \quad (1)$$

Here r is the radial distance in a cylindrical coordinate system. Assuming Z_0 is the distance between the lens L_1 in Fig. 1 and the EB waist location, $\omega^2(Z) = \omega_e^2 + [\lambda_e(Z - Z_0)/(\pi\omega_e)]^2$. Here λ_e is the EB wavelength. The power through the pinhole at the centre of the EB becomes

$$P_{de}(Z) = 2\pi \int_0^{d/2} I(r,Z) r dr = P_e \left\{1 - exp\left[-\frac{d^2/2}{\omega_e^2 + [\lambda_e(Z-Z_0)/(\pi\omega_e)]^2}\right]\right\}. \quad (2)$$

Eq. (2) was used for the curve fitting to find ω_e and Z_0, and Fig. 2(a) displays a typical measurement result. Three measurements were performed, and the ω_e was found to be (4.87 ± 0.01) × 10^{-5} m as the average.

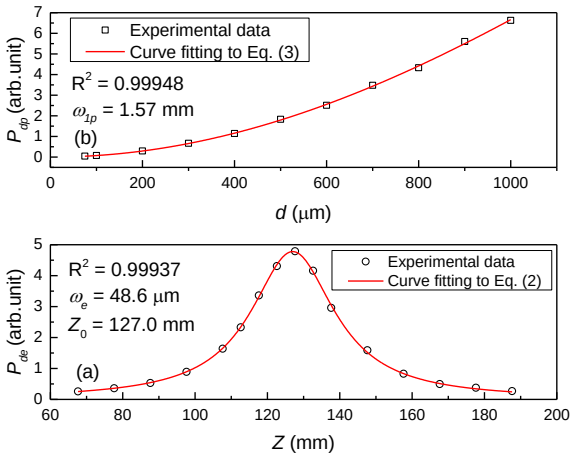

FIG. 2. Typical experimental data and least-squares curve fittings of the measurements of EB and PB spot size at the sample position: (a) EB spot size measurement, (b) PB spot size measurement

The radius ω_{1p} of the PB at the EB waist (i.e. the sample position) was also measured. The abovementioned pinhole-detector assembly was put at the EB waist position. The power P_{dp} through the pinhole at the centre of the Gaussian PB can be expressed as

$$P_{dp} = P_p \left\{1 - exp\left[-\frac{d^2/2}{\omega_{1p}^2}\right]\right\}. \quad (3)$$

Here P_p is the total power of the EB. A curve of P_{dp} against d could be created by measuring the P_{dp} with the pinholes of different diameters d. The ω_{1p} could be obtained by fitting the $P_{dp} \sim d$ curve to Eq. (3), as shown in Fig. 2(b). As the average of four measurements, the PB spot size ω_{1p} at the sample position was found to be $\omega_{1p} = (1.56 \pm 0.02) \times 10^{-3}\, m$.

With the forgoing configurations, steady-state TL signals varying with the EB power were measured with deionized water as a sample in a 10-mm thick quartz cuvette (PerkinElmer). The experimental results were compared with the theoretical calculation using the model presented in Ref. 11.

III. Results and discussion

According to a theoretical model for the TL experiment arrangement as shown in Fig. 3, the time-resolved PB intensity (transient) $I_p(t)$ at its beam centre at the detector plane is[11]

$$I_p(t) = I_p(0)\left(1 - \frac{\theta}{2} tan^{-1}\left\{\frac{2mV}{[(1+2m)^2+V^2][t_c/(2t)]+1+2m+V^2}\right\}\right)^2. \quad (4)$$

In Eq. (4), $\theta = -\frac{P_e b l}{k\lambda_p}\frac{dn}{dT}$, $t_c = \omega_e^2/(4D)$, $m = \left(\omega_{1p}/\omega_e\right)^2$, and $V = \frac{\pi\omega_{1p}^2}{\lambda_p}\left(\frac{1}{R_{1p}} + \frac{1}{Z_2}\right)$. Here b, l, $\frac{dn}{dT}$, k, D, denote the linear absorption (attenuation) coefficient at the excitation beam wavelength λ_e, sample thickness, thermo-optic coefficient (namely, the temperature coefficient of the refractive index) at the PB wavelength λ_p, thermal conductivity, and thermal diffusivity of the sample respectively.

R_{1p} and Z_2 are the radius of curvature of the PB at the sample location and the distance between the sample and the detector plane (e.g., the location of the pinhole-photodiode assembly in Fig. 1) respectively. When the PB is a collimated Gaussian laser beam, $R_{1p} \to \infty$, and therefore $V = \frac{\pi\omega_{1p}^2}{\lambda_p Z_2}$. $I_p(0)$ is the PB intensity at the absence of the TL.

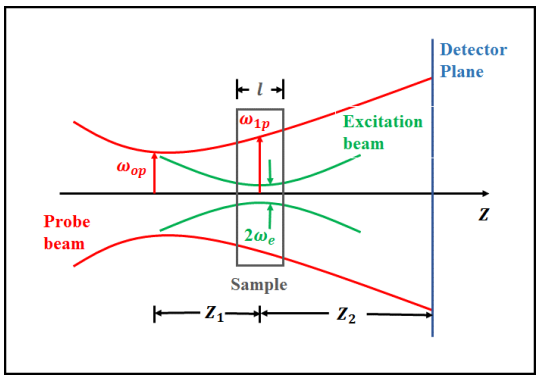

FIG. 3. Scheme of the geometric positions of laser beams in a conventional mode-mismatched dual-beam TL experimental arrangement.

When the measurement time $t \gg t_c$, the steady-state TL signal S can be defined as[11]

$$S = \frac{I_p(\infty) - I_p(0)}{I_p(0)} = \left[1 - \frac{\theta}{2}\tan^{-1}\left(\frac{2mV}{1+2m+V^2}\right)\right]^2 - 1. \quad (5)$$

If $\left|\frac{\theta}{2}\tan^{-1}\left(\frac{2mV}{1+2m+V^2}\right)\right| \ll 1$, Eq. (5) becomes

$$S = -\theta\tan^{-1}\left(\frac{2mV}{1+2m+V^2}\right) = \frac{P_e b l}{k\lambda_p}\frac{dn}{dT}\tan^{-1}\left(\frac{2mV}{1+2m+V^2}\right). \quad (6)$$

Numerical calculation reveals that if $\left|\frac{\theta}{2}\tan^{-1}\left(\frac{2mV}{1+2m+V^2}\right)\right| < 0.1$, 0.04, or 0.001 the relative difference between Eqs. (5) and (6) is smaller than 5.27%, 2.05%, or 0.503% respectively. For the new configuration probing the TL twice, as shown in Fig. 1(b), the steady-state TL signal S' can be expressed as[14]

$$S' = \frac{2P_e bl}{k\lambda_p}\frac{dn}{dT}\tan^{-1}\left(\frac{2mV}{1+2m+V^2}\right). \quad (7)$$

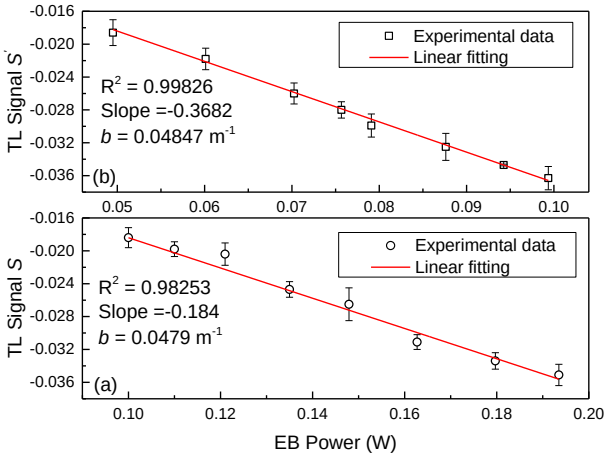

FIG. 4. Typical experimental data and linear fitting of the steady-state TL signals versus different EB power with (a) conventional configuration (probing TL once), (b) new configuration (probing TL twice)

TABLE I. Parameters used for the computation of Eqs. (6) and (7)

Sample thickness $\boldsymbol{l}$	10^{-2} m
EB (532.3 nm) radius at sample $\boldsymbol{\omega_e}$	$(4.87 \pm 0.01) \times 10^{-5}$ m
PB (632.992 nm) radius at sample $\boldsymbol{\omega_{1p}}$	$(1.56 \pm 0.02) \times 10^{-3}$ m
$\boldsymbol{m}$	1.03×10^{3}
$\boldsymbol{V}$	12.08
$\boldsymbol{Z_2}$	1 m
thermo-optic coefficient $\frac{\boldsymbol{dn}}{\boldsymbol{dT}}$ of water at 632.8 nm[15]	-9.7×10^{-5} K^{-1}
Thermal conductivity $\boldsymbol{k}$ of water[16]	0.598 W m^{-1} K^{-1}

Eqs. (6) and (7) indicate that the steady-state TL signal is linearly proportional to P_e and the linear absorption (attenuation) coefficient b at wavelength λ_e can be quantitatively deduced from the signal if all other parameters in the equations are well-known. Fig. 4 presents typical TL

signal varying with various EB power and consequent linear fitting. Consequently, the average slopes (sensitivities) of three measurements with the conventional and new configurations are found to be -0.180 ± 0.009 and -0.372 ± 0.004 respectively. Taking the standard deviations into account, the slope with the new configuration is twice of that with the conventional one, which is consistent with Eqs. (6) and (7). The consistency makes it possible to quantify the linear absorption (attenuation) coefficient b of deionized water at 532.3 nm by linear fitting to Eqs. (6) and (7) with the parameters listed in Table I. b = (4.7 ± 0.2) × 10^{-2} m^{-1} and b = (4.90 ± 0.05) × 10^{-2} m^{-1} are thus determined, respectively, with the conventional and new configurations. The b values thus obtained are in good agreement with the literature value (4.5 ± 0.2) × 10^{-2} m^{-1} at 532.5 nm determined by an integrating cavity technique.[17] The b values also agree with the literature values 4.27 × 10^{-2} m^{-1} at 531.8 nm and 4.39 × 10^{-2} m^{-1} at 534.7 nm measured with pulsed optoacoustic spectroscopy and estimated as ±10% in the accuracy.[18] Considering the standard deviations, one may notice that these two b values attained in this work are essentially the same. Furthermore, the precision of the b measured with the new configuration is higher than that measured with the conventional one.

Examination of Eqs. (6) and (7) exhibits that the TL signal enhancement with the new configuration is mathematically equivalent to doubling the sample thickness in a conventional configuration. However, in practice, this signal enhancement is not always achievable by doubling the sample thickness. The theoretical model in Ref. 11 was developed with some assumptions. One of them is that the sample thickness is less than the confocal distances of both the EB and PB to ensure the beam spot sizes are constant through the sample. Usually, in a mode-mismatched TL experiment, the focal distance of the EB is shorter than that of the PB. Since the focal distance Z_{ce} of the EB depends on ω_e^2

$$Z_{ce} = \frac{\pi \omega_e^2}{\lambda_e}, \tag{8}$$

a longer Z_{ce} for accommodating a thicker sample requires a larger EB spot size ω_e. On the other hand, the increase of ω_e causes the decrease of the phase shift Φ on the PB wavefront, as indicated by the following eqation[11]

$$\Phi(r,t) = \frac{\theta}{t_c}\int_0^t \frac{1}{1+2t'/t_c}\left[1 - exp\left(-\frac{2r^2/\omega_e^2}{1+2t'/t_c}\right)\right]dt', \quad (9)$$

resulting in the decrease of TL signal and, in effect, the sensitivity. With the new configuration the TL signal and sensitivity are doubled without increasing the EB spot size, and therefore the sensitivity enhancement is greater than that by simply doubling the sample thickness in a conventional configuration.

IV. Conclusions

In this work a mode-mismatched TL configuration probing TL twice has been developed. Compared with the conventional configuration (probing TL once), the TL signal and sensitivity with this new configuration is doubled as predicted by the theoretical model, which is better than the effect of simply doubling the sample thickness in a conventional configuration. Also, the absorption coefficient of deionized water can be precisely measured, which is in good agreement with the literature values. This new TL configuration can be used in the areas requiring high sensitivity, e.g., ultra-trace analysis.

Acknowledgement

Support from the Office of Energy Research and Development (OERD), Natural Resources Canada, Government of Canada is gratefully acknowledged.

Data Availability

The data that support the findings of this study are available from the corresponding author upon reasonable request.

REFERENCES

[1] S. E. Bialkowski, N. G. C. Astrath, M. A. Proskurnin, "Photothermal spectroscopy methods," 2nd Edition, John Wiley & Sons, New York (2019).

[2] J. Shen, K. H. Michaelian, R. Gieleciak, M. L. Baesso, N. G. C. Astrath, L. C. Malacarne, J. Appl. Phys. **128**, 190902 (2020).

[3] J. Shen, R. D. Snook, Chem. Phys. Lett. **155**, 583 (1989).

[4] M. L. Baesso, J. Shen, R. D. Snook, Chem. Phys. Lett. **197**, 255 (1992).

[5] J. Shen, R. D. Snook, Analytical Proceedings **26**, 403 (1989).

[6] R. A. Cruz, A. Marcano, C. Jacino, T. Catunda, Opt. Lett. **34**, 1882 (2009).

[7] C. Hu, J. R. Whinnery, Appl. Opt. **12**, 72 (1973).

[8] M. E. Long, R. L. Swofford, A. C. Albrecht, Science **191**, 183 (1976).

[9] T. Higashi,T. Imasaka, N. Ishitoashi, Anal. Chem. **55**, 1907 (1983).

[10] T. Berthoud, N. Delorme, P. Mauchien, Anal. Chem. **57**, 1217 (1985).

[11] J. Shen, R. D. Lowe, R. D. Snook, Chem. Phys. **165**, 385 (1992).

[12] R. Silva, M. A. C. de Araújo, P. Jali, S. G. C. Moreira, P. Alcantara Jr., P. C. de Oliveira, AIP Advances **1**, 022154 (2011).

[13] A. Marcano, H. Cabrera, M. Guerra, R. A. Cruz, C. Jacinto, T. Catunda, J. Opt. Soc. Am. B **23**, 1408 (2006).

[14] H. Cabrera, L. Goljat, D. Korte, E. Marin, M. Franko, Anal. Chim. Acta **1100**, 182 (2020).

[15] J. Zhou, J. Shen, W. S. Neill, Rev. Sci. Instrum. **87**, 073104 (2016).

[16] S. E. Bialkowski, "Photothermal Spectroscopy Methods for Chemical Analysis," 1st Edition, John Wiley & Sons, New York (1996).

[17] R. M. Pope, E. S. Fry, Appl. Opt. **36**, 8710 (1997).

[18] C. K. N. Patel, A. C. Tam, Rev. Mod. Phys. **53**, 517 (1981).